Inorganica Chimica Acta 394 (2013) 415–422

Contents lists available at SciVerse ScienceDirect

Inorganica Chimica Acta

journal homepage: www.elsevier.com/locate/ica

Copper(II) complexes of symmetric and asymmetric bis(imine) ligands: Tuning the Cu(I)/Cu(II) redox couple

Anna Jozwiuk [a], Zhaodong Wang [a], Douglas R. Powell [a], Robert P. Houser [a,b,*]

[a] Department of Chemistry and Biochemistry, University of Oklahoma, Norman, OK 73019, United States
[b] Department of Chemistry and Biochemistry, University of Northern Colorado, Greeley, CO 80639, United States

ARTICLE INFO

Article history:
Received 4 May 2012
Received in revised form 27 August 2012
Accepted 28 August 2012
Available online 15 September 2012

Keywords:
Copper complexes
X-ray crystal structures
Electrochemistry

ABSTRACT

Two new pyridylbis(imine) ligands 2-((2-methyl-2-(pyridin-2-yl)-3-(pyridin-2-ylmethyleneamino) propylimino)methyl)phenol, HL^2, and 2-methyl-2-(pyridin-2-yl)-N^1,N^3-bis(pyridin-2-ylmethylene) propane-1,3-diamine, L^3, were synthesized via the Schiff base condensation of 2-methyl-2-pyridin-2-yl-propane-1,3-diamine and either 2-pyridinecarboxaldehyde or 2-hydroxybenzaldehyde. Complexation of Cu(II) ions by HL^2 and L^3 yielded $[Cu(HL^2)]_2(ClO_4)_4$ (**2**), and $[Cu(L^3)](ClO_4)_2$ (**3**), respectively. The structures and electrochemistry of **2** and **3** were compared to our previously synthesized Cu(II) complex of the ligand 2,2'-(2-methyl-2-(pyridin-2-yl)propane-1,3-diyl)bis(azan-1-yl-1-ylidene)bis(methan-1-yl-1-ylidene)diphenol (H_2L^1), which coordinates to Cu(II) as a dianion to form $[Cu(L^1)(CH_3OH)]$ (**1**). Whereas $(L^1)^{2-}$ and L^3 form mononuclear complexes with Cu(II) ions, the asymmetric ligand HL^2 produces copper dimers in the solid state with the phenolate O atoms bridging between copper ions. Solution magnetic moment measurements and ESI–MS suggest that all three species exist as monomers in solution, although small amounts of dimeric **2** were detected in solution by ESI–MS and EPR spectroscopy. Complexes of all three ligands show similar EPR properties with typical axial spectra. Cyclic voltammetry reveals that the Cu(I)/Cu(II) redox couples of **2** and **3** are shifted to more positive potentials than that of **1**, with **3** having the most positive one-electron reduction potential: $E_{1/2}(\mathbf{1}) = -1.489$ V; $E_{1/2}(\mathbf{2}) = -1.099$ V; $E_{1/2}(\mathbf{3}) = -0.438$ V, all versus Fc/Fc^+.

1. Introduction

Copper is one of the most abundant redox active metals and plays an important role in many biological processes. For example, blue copper electron transfer proteins use copper as a one electron relay, shuttling between the cuprous and cupric oxidation states [1]. The tuning of the Cu^{II}/Cu^{I} redox couple is a critical component of electron transfer in blue copper proteins, and is also important in synthetic complexes where copper plays a role as the redox center in catalysis [2,3]. The relationship between redox potential and structure has therefore received considerable attention for many years [4–8]. While geometric constraints, e.g. tetrahedral versus square planar copper in blue copper proteins, are of great importance, ligand donor atoms are also a key factor in redox potential. Sigma- and pi-donor ligands push more electron density on the metal ion, moving the CuII/I redox potential to lower (more negative) potentials [9].

Copper complexes with chelating Schiff base ligands have been thoroughly investigated. Schiff bases are important ligands because of their simplicity in syntheses and the diversity of possible ligands owing to the mix-and-match ability of the condensation of various amines with different aldehydes. In particular, tetradentate Schiff base ligands, including salen and its derivatives, have been used for a wide variety of coordination chemistry with copper and other transition metals [10–17]. Generally, the salen-type ligands coordinate to copper in a square-planar mode (see Fig. 1). The syntheses of tetradentate Schiff base ligands are versatile due to their modular nature. An alkanediamine backbone starting material can easily be transformed into a tetradentate ligand by condensation with two equivalents of an aldehyde.

Examples of how different tetradentate Schiff base donors influence the Cu^{II}/Cu^{I} redox potential of the corresponding complex have been reported in the literature [16,18–21]. It has been shown that the length of the alkane chain of the diamine unit plays an important role in the redox behavior of the metal ion, as this type of ligand variation selects for different coordination geometries, (e.g. tetrahedral versus square planar) [18,19]. In a different study, variation of the weakly coordinated counterion in the axial position of the quadridentate Schiff base copper complex influences the electrochemistry of the copper couple [20]. Although diamines

* Corresponding author at: Department of Chemistry and Biochemistry, University of Northern Colorado, Greeley, CO 80639, United States. Tel.: +1 970 351 2877; fax: +1 970 351 2176.
E-mail address: robert.houser@unco.edu (R.P. Houser).

0020-1693/$ - see front matter © 2012 Elsevier B.V. All rights reserved.
http://dx.doi.org/10.1016/j.ica.2012.08.026

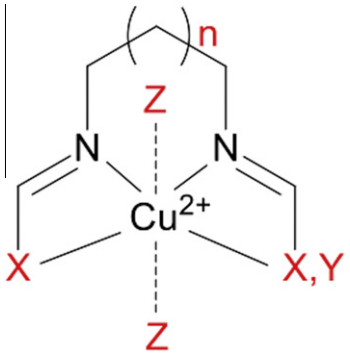

Fig. 1. General structure of copper(II) complexes with tetradentate Schiff base ligands. X, Y = donor group (e.g. pyridyl or phenolate), Z = counterion in axial position and n = number of $-(CH_2)-$ units.

should allow stepwise condensation of two different aldehydes and therefore more variation, not much has been reported on the electrochemistry of copper complexes with these ligands. Ghosh and coworkers have shown that the monocondensed product of 1,3-propanediamine and 1-benzoylacetone can be used as a precursor for condensation with 2-pyridinecarboxaldehyde or 2-acetylpyridine [20]. These asymmetric copper complexes show drastic shifts in redox potentials of the copper ion compared to the symmetric condensation product of 1,3-propanediamine with two equivalents of 1-benzoylacetone [21]. The asymmetric copper complex of 1:1:1 condensation of 1,3-propanediamine, 2,4-pentanedione and 2-pyridinecarboxaldehyde showed irreversible reductions and the copper complexes readily reorganized into its symmetric complexes in the presence of catalytic amounts of acid and copper(II) ions [16].

In this paper we contrast the electrochemical properties of copper(II) complexes of three related tetradentate Schiff base ligands, H_2L^1, HL^2, and L^3. Recently we reported the synthesis of a symmetric Schiff base ligand H_2L^1 (Fig. 2), derived from 2-methyl-2-pyridin-2-yl-propane-1,3-diamine (ppda) and 2-hydroxybenzaldehyde [22]. Herein we report the synthesis of the more electron deficient bis(pyridyl) bis(imine), L^3, and the asymmetric hybrid version containing both a pyridyl group and a phenol group, namely HL^2 (see Fig. 2). The latter ligand allows access to intermediate electronic properties between the two strictly symmetric ligands.

2. Experimental

2.1. Abbreviations

ppda = 2-methyl-2-pyridin-2-yl-propane-1,3-diamine; H_2L^1 = 2,2′-(2-methyl-2-(pyridin-2-yl)propane-1,3-diyl)bis(azan-1-yl-1-ylidene)bis(methan-1-yl-1-ylidene)diphenol; HL^2 = 2-((2-methyl-2-(pyridin-2-yl)-3-(pyridin-2-ylmethyleneamino)propylimino)methyl)phenol; L^3 = 2-methyl-2-(pyridin-2-yl)-N^1,N^3-bis(pyridin-2-ylmethylene)propane-1,3-diamine; **1** = $[Cu(L^1)(CH_3OH)]$; **2** = $[Cu(HL^2)]_2(ClO_4)_4$; **3** = $[Cu(L^3)](ClO_4)_2$.

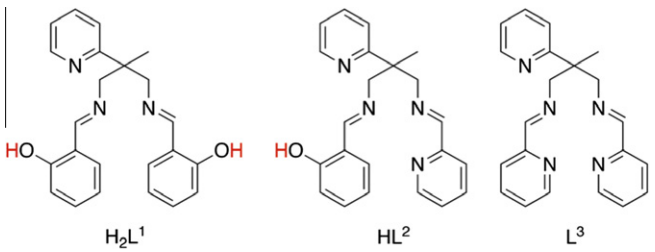

Fig. 2. Structures of the previously synthesized ligand H_2L^1 and the two new ligands HL^2 and L^3. Ionizable protons are highlighted in red. (For interpretation of the references to colour in this figure legend, the reader is referred to the web version of this article.)

2.2. General procedures

Unless otherwise stated, all reagents were used as received from commercial sources. 2-Methyl-2-(pyridine-2-yl)propane-1,3-diamine (ppda) was synthesized according to the published procedure [23]. H_2L^1 and **1** were synthesized according to the published procedures [22]. Solvents used were doubly purified using alumina columns in a MBraun solvent purification system (MB-SPS). Infrared spectra were measured from 4000 to 400 cm^{-1} as KBr pellets on a BIO-RAD FTS 155 FTIR spectrometer. ^1H NMR spectra were measured using a Varian 300 MHz instrument using solvent ($CHCl_3$) as an internal standard. Mass spectra were measured on a Q-TOF quadrupole time-of-flight mass spectrometer (Micromass, Manchester, UK) equipped with a Z-spray electrospray ionization (ESI) source. Elemental analyses were performed by Atlantic Microlab, Norcross, GA. UV–Vis spectra were measured using a Shimadzu UV2401PC spectrophotometer in the range 250–900 nm on solutions ranging in concentration from 1.0×10^{-3} to 1.0×10^{-4} M. Cyclic voltammetry experiments were performed using a BAS 50 W potentiometer and a standard three-electrode cell with a glassy-carbon working electrode, a Pt-wire auxiliary electrode, and an Ag/AgCl pseudo-reference electrode under an inert atmosphere at room temperature. X-band EPR spectra of the complexes were recorded at 77 K using a Bruker EMX spectrometer. Magnetic susceptibilities of the complexes in the solid state were measured at 295 K using a Johnson Matthey magnetic susceptibility balance (MSB – AUTO) with a magnetic field strength of 4.5 kGauss and a measurement range of $\pm 1.999 \times 10^{-4}$ to $\pm 5 \times 10^{-10}$ cgs. Solution magnetic susceptibilities were measured at 294 K by the Evans method [24].

Caution: Perchlorate salts of metal complexes with the organic ligands are potentially explosive. Although no difficulty was encountered during the syntheses described herein, they should be prepared in small amounts and handled with caution.

2.3. HL^2

2-Pyridinecarboxaldehyde (0.127 g, 1.15 mmol) was added dropwise to a solution of ppda (0.190 g, 1.15 mmol) in CH_3OH (5 mL). The resulting yellow solution was refluxed overnight, causing a color change to light orange. The solvent was removed in vacuo to give L^4 as an orange-brown oil (0.290 g). ^1H NMR (300 MHz, DMSO-d^6, 293 K) δ 1.02–1.44 (m, 3H), 2.89–4.51 (m, 4H), 4.47–4.54 (m, 1H), 7.18–7.90 (m, 6H), 8.27–8.62 (m, 2H). See Supporting information, Fig. S5. Crude L^4 was redissolved in CH_3OH (5 mL) without further purification, and 2-hydroxybenzaldehyde (0.136 g, 1.11 mmol) was added. While refluxing overnight the solution turned light green. The solvent was removed in vacuo, yielding HL^2 as a highly viscous orange oil (0.400 g). The oil was kept under nitrogen and solidified after several months. According to NMR spectroscopy the composition of the ligand did not change upon solidification. ^1H NMR (300 MHz, $CDCl_3$, 293 K) δ 1.54 (m, 3H), 3.95–4.30 (m, 4H), 6.78–6.93 (m, 2H), 7.05–7.43 (m, 5H), 7.55–7.74 (m, 2H), 7.92–7.99 (m, 1H), 8.26–8.37 (m, 2H), 8.56–8.66 (m, 2H), 13.14–13.34 (m, 1H).). ESI–MS (CH_3OH): m/z = 359.2 $[HL^2 + H]^+$, 255.2 $[L^4 + H]^+$ (minor). Solutions of HL^2 decompose within hours, probably due to hydrolysis in the presence of moisture (see Supporting information, Fig. S2). Due to the highly viscous, sticky nature of the ligand, no elemental analysis was

performed. Purification was achieved through complex formation with copper(II) ions.

2.4. L^3

2-Pyridinecarboxaldehyde (0.363 g, 3.39 mmol) was added dropwise to a solution of ppda (0.280 g, 1.69 mmol) in CH_3OH (5 mL). The resulting yellow solution was refluxed overnight, causing a color change to light orange. The solvent was removed in vacuo to give the ligand as a highly viscous dark orange oil (0.575 g). ^1H NMR (300 MHz, $CDCl_3$, 293 K) δ 1.55 (s, 3H), 4.12–4.24 (m, 4H), 7.05–7.11 (m, 1H), 7.24–7.30 (m, 2H), 7.37–7.42 (m, 1H), 7.55–7.62 (m, 1H), 7.64–7.72 (m, 2H), 7.92–7.98 (m, 2H), 8.32–8.37 (m, 2H), 8.57–8.63 (m, 3H). ESI–MS (CH_3OH): m/z = 344.2 $[L^3 + H]^+$, 255.2 $[L^4 + H]^+$. Solutions of L^3 decompose within hours, probably due to hydrolysis in the presence of moisture (see Supporting information, Fig. S3). Due to the highly viscous, sticky nature of the ligand, no elemental analysis was performed. Purification was achieved through complex formation with copper(II) ions.

2.5. $[Cu(HL^2)]_2(ClO_4)_4$ (**2**)

$Cu(ClO_4)_2{\cdot}6H_2O$ (0.220 g, 0.586 mmol) dissolved in methanol (1 mL) was added to a solution of ligand HL^2 (0.210 g, 0.586 mmol) in CH_3OH (10 mL). The resulting dark green solution was stirred overnight at room temperature to yield an olive-green precipitate which was isolated by filtration, washed with methanol and diethylether (0.200 g, 53%). *Anal.* Calc. for **2**·$2H_2O$, powder, $C_{44}H_{48}Cl_4Cu_2N_8O_{20}$: C, 41.36; H, 3.79; N, 8.77. Found: C, 41.47; H, 3.51; N, 8.83%. X-ray quality crystals were obtained from Et_2O diffusion into a solution of **2** in methanol/acetonitrile. *Anal.* Calc. for **2**, crystals, $C_{44}H_{44}Cl_4Cu_2N_8O_{18}$: C, 42.56; H, 3.57; N, 9.02. Found: C, 42.08; H, 3.86; N, 9.41%. UV/Vis (CH_3CN) [λ_{max}, nm (ε, $M^{-1}\,cm^{-1}$)]: 243 (18300), 272 (15600), 369 (5,470), 573 (128). EPR (9.468 GHz, mod. amp. 25.0 G, CH_3CN, 77 K): $g_{||}$ = 2.19, $g_{\perp}$ = 2.06, and $A_{||}$ = 205 G. EPR (9.466 GHz, mod. amp. 25.0 G, CH_3OH, 77 K): $g_{||}(1)$ = 2.22, $g_{\perp}(1)$ = 2.04, and $A_{||}(1)$ = 190 G; $g_{||}(2)$ = 2.31, $g_{\perp}(2)$ = 2.04, and $A_{||}(2)$ = 200 G. FTIR (KBr): 2364, 2343, 1616, 1537, 1468, 1448, 1402, 1328, 1301, 1106, 1089, 1030, 964, 780, 768, 624, 533, 508, 417 cm^{-1}. ESI–MS (CH_3CN or CH_3OH): m/z = 420.1 $[Cu(L^2)]^+$, 941.1 $[(Cu(L^2))_2ClO_4]^+$. Solid state magnetic moment (MSB-Auto, 4.5 kG, 22.0 °C): 4.4 μ_B. Solution magnetic moment (Evans method, 20.9 °C, 16.3 × 10^{-3} M, acetonitrile-d_3): 1.76 μ_B.

2.6. $[Cu(L^3)](ClO_4)_2$ (**3**)

2-Pyridinecarboxaldehyde (0.027 g, 0.254 mmol) was added dropwise to a solution of hexahydropyrimidine (0.065 g, 0.254 mmol) in CH_3OH (5 mL) and the reaction mixture refluxed for 3 h. After cooling to room temperature $Cu(ClO_4){\cdot}6H_2O$ (0.094 g, 0.254 mmol) in methanol (1 mL) was added. The resulting turquoise solution was stirred overnight at room temperature to yield a light blue precipitate which was isolated by filtration, washed with methanol, diethylether and pentane (0.120 g, 78%). X-ray quality crystals were obtained from Et_2O diffusion into a solution of **3** in acetonitrile. *Anal.* Calc. for $C_{21}H_{21}Cl_2CuN_5O_8$: C, 41.63; H, 3.49; N, 11.56. Found: C, 41.89; H, 3.54; N, 11.64. UV/Vis (CH_3CN) [λ_{max}, nm (ε, $M^{-1}\,cm^{-1}$)]: 281 (15900), 661 (117). EPR (9.441 GHz, mod. amp. 25.0 G, CH_3CN, 77 K): $g_{||}$ = 2.19, $g_{\perp}$ = 2.07 and $A_{||}$ = 185 G. FTIR (KBr): 2364, 2343, 1653, 1602, 1564, 1475, 1429, 1311, 1267, 1230, 1121, 1090, 1023, 981, 954, 787, 760, 671, 622, 502, 420 cm^{-1}. ESI–MS (CH_3CN): m/z = 505 $[Cu(L^3)ClO_4]^+$. Solid state magnetic moment (MSB-Auto, 4.5 kG, 22.0 °C): 3.5 μ_B. Solution magnetic moment (Evans method, 20.9 °C, 16.8 × 10^{-3} M, acetonitrile-d_3): 1.75 μ_B.

Table 1
Crystallographic data for **2** and **3**.

	2·$2CH_3OH$	**3**
Formula	$C_{46}H_{52}Cl_4Cu_2N_8O_{20}$	$C_{21}H_{21}Cl_2CuN_5O_8$
fw	1305.84	605.87
Crystal system	Monoclinic	Triclinic
Space group	*C*2/*c*	*P*–1
Unit cell dimensions		
a (Å)	20.587(12)	9.183(4)
b (Å)	12.266(7)	10.365(4)
c (Å)	21.779(12)	12.064(5)
α (deg)	90	88.416(8)
β (deg)	110.162(16)	84.424(10)
γ (deg)	90	85.125(12)
V (Å^3)	5163(5)	1138.5(8)
Z	4	2
$\rho_{Calc.}$ (mg/m^3)	1.680	1.767
μ (mm^{-1})	1.119	0.71073
θ (°)	1.97 to 28.52	1.70 to 28.42°
R_1,[a] wR_2[b] [$I > 2\sigma(I)$]	0.0456, 0.1118	0.0553, 0.1359
Goodness-of-fit (GOF) on F^2	1.001	1.001

[a] $R1 = \Sigma||F_{obs}| - |F_{calc}||/\Sigma|F_{obs}|$.
[b] $wR^2 = \{\Sigma[w(F_{obs}{}^2 - F_{calc}{}^2)^2]/\Sigma[w(F_{obs}{}^2)^2]\}^{1/2}$.

2.7. X-ray crystal structure determination

Intensity data for **2** and **3** were collected using a diffractometer with a Bruker APEX ccd area detector [25,26]. Data were collected using graphite-monochromated Mo Kα radiation (λ = 0.71073 Å). The samples were cooled to 100(2) K. Cell parameters were determined from a non-linear least squares fit of the data. The data were corrected for absorption by the semi-empirical method [27]. The structures were solved by direct methods and refined by full-matrix least-squares methods on F^2 [28,29]. Hydrogen atom positions of hydrogens bonded to carbons were initially determined by geometry and refined by a riding model. Hydrogens bonded to nitrogens or oxygens were located on a difference map, and their positions were refined independently. Non-hydrogen atoms were refined with anisotropic displacement parameters. Hydrogen atom displacement parameters were set to 1.2 (1.5 for methyl) times the displacement parameters of the bonded atoms. Crystal data for **2** and **3** are summarized in Table 1. Selected bond lengths and angles for **2** and **3** are summarized in Table 2. Hydrogen bonding information of **2** is represented in Table 3.

3. Results and discussion

3.1. Syntheses

3.1.1. Ligands

The previously reported ligand H_2L^1 (Fig. 2) was prepared through Schiff base condensation of ppda with 2-hydroxybenzaldehyde, and isolated in high yields in our laboratory [22]. Using the same approach, two novel ligands HL^2 and L^3 (see Fig. 2) were synthesized. HL^2 is a potentially monoanionic ligand with an N_4O donor set, whereas L^3 is neutral with an N_5 donor set. HL^2 and L^3 were synthesized via condensation of ppda with one equivalent each of 2-pyridinecarboxaldehyde and 2-hydroxybenzaldehyde, or two equivalents of 2-pyridinecarboxaldehyde, respectively. However, we were not able to obtain HL^2 and L^3 in high purity.

There are challenges in the synthesis of asymmetric ligands like HL^2, such as the step-wise condensation of different aldehydes with the diamine starting material. Some examples of asymmetric bis(imine) and bis(amine) ligands, as well as their metal complexes can be found in the literature [30–34]. An additional difficulty that must be taken into account in the step-wise condensation of 1,3-propanediamine units with two different aldehydes is the ten-

Table 2
Selected bond lengths (Å) and angles (deg) for **2** and **3**.

Complex **2**			
Cu1–O1	1.922(2)	Cu1–N9	1.956(3)
Cu1–N20	2.020(2)	Cu1–N27	2.010(3)
Cu1–O1#1	2.487(2)	Cu1–O2A	2.763(3)
O1–Cu1–N9	94.22(9)	O1–Cu1–N27	91.35(9)
N9–Cu1–N20	93.97(9)	N27–Cu1–N20	80.94(9)
N9–Cu1–N27	169.94(9)	O1–Cu1–N20	171.38(9)
O1–Cu1–O1#1	82.52(8)	N27–Cu1–O1#1	89.87(8)
N9–Cu1–O1#1	99.14(8)	N20–Cu1–O1#1	93.55(8)
Complex **3**			
Cu1–N19	1.966(2)	Cu1–N8	1.996(2)
Cu1–N1	2.018(2)	Cu1–N22	2.050(2)
Cu1–O1B	2.573(2)	Cu1–O1A	2.660(2)
N19–Cu1–N8	91.65(9)	N19–Cu1–N1	168.37(9)
N8–Cu1–N1	82.63(9)	N19–Cu1–N22	81.35(9)
N8–Cu1–N22	169.95(9)	N1–Cu1–N22	105.50(9)
N19–Cu1–O1B	106.80(9)	N8–Cu1–O1B	85.17(8)
N1–Cu1–O1B	82.89(9)		

Symmetry information used to generate equivalent positions: $(-x + ½, -y + ½, -z)$.

Table 3
Hydrogen bonds (Å) and angles (deg) for **2**.

D–H···A	d(D–H)	d(H···A)	d(D···A)	<(DHA)
N14–H14···O1S	0.83(3)	2.01(3)	2.764(3)	151(3)
O1S–H1S···O1A#2	0.74(4)	2.24(4)	2.864(3)	144(4)

Symmetry information used to generate equivalent positions: $(-x + ½, -y + ½, -z)$.

dency in formation of hexahydropyrimidines (through cyclization) with the first equivalent of aldehyde [35]. The advantage of the cyclization, though, is the directed yield in mono condensed products over a mix of doubly condensed and unreacted species. The most challenging aspect is the hydrolysis of asymmetric bis(imine)s followed by condensation to their symmetric analogues. However, this problem can be overcome by metal chelation, which prevents decomposition and rearrangement.

Our attempts to purify L^3 through chromatography (silica, CH_2Cl_2:CH_3OH, 95%/5%) resulted in its decomposition. The two collected fractions were identified as 2-pyridinecarboxaldehyde and a mixture of compounds (the majority being most likely the cis and trans isomers of the hexahydropyrimidine L^4: see Scheme 1 and the ^1H NMR spectrum in Figure S4). In addition, we observed decomposition of both ligands HL^2 and L^3 in solution over time, to 2-pyridinecarboxaldehyde and possibly the hexahydropyrimidine species, which was indicated by the growth in the ^1H NMR of the aldehydic proton of 2-pyrdinecarboxaldehyde signal, and the appearance of additional signals in the methyl, methylene and aromatic regions. ^1H NMR spectra of solutions of H_2L^1, HL^2 and L^3, taken immediately and taken after four days are shown in the Supporting information, Figs. S1–S3, respectively. The spectrum of H_2L^1 only shows a growth in the water peak signal while HL^2 and L^3 show decomposition.

Our observations on the instability of ligands HL^2 and L^3 are in good agreement with recently published work on the formation of bis(imine)s and hexahydropyrimidines via the condensation of 1,3-propanediamine with various aldehydes. Locke et al. reported the preference of the formation of hexahydropyrimidines with electron deficient aldehydes (e.g. 2-pyridinecarboxaldehyde), and the tendency to form bis(imine)s with electron rich aldehydes like 2-hydroxybenzaldehyde [35]. The electron withdrawing nature of the pyridine ring in 2-pyridinecarboxaldehyde seems to induce the formation of a hexahydropyrimidine rather than an imine with the 1,3-propanediamine unit [35]. Also, the potential for the formation of intramolecular hydrogen bonds between the phenol hydrogen atoms and the imine nitrogen atoms in H_2L^1 may stabilize the bis(imine) while L^3 cannot develop similar hydrogen bonding.

3.1.2. Copper complexes

Despite difficulties in isolating HL^2 and L^3, we were able to obtain pure metal complexes of the two ligands upon coordination to copper(II) salts. A methanolic solution of either crude HL^2 or L^3 was typically treated with copper(II) perchlorate to yield **2** or **3** as olive-green and light blue precipitates, respectively (Scheme 1a and e). Complex **3** was also obtained when L^3 was generated in situ from L^4 in solution, along with one equivalent of 2-pyridinecarboxaldehyde followed by subsequent addition of cupric perchlorate as shown in Scheme 1f. Crystals suitable for X-ray structural analysis were obtained after recrystallization of the powders. Complex **2** was found in the solid state to be a dimeric species of two $[Cu(HL^2)]^{2+}$ subunits where the proton on the phenol group has migrated to the pyridyl N atom, namely $[Cu(HL^2)]_2(ClO_4)_4$. The ligand in complex **2** is therefore still neutral despite the deprotonated phenolate due to the protonated pyridinium group. In contrast to **2**, complex **3** was isolated as a monomer $[Cu(L^3)](ClO_4)_2$. Solutions of **2** in methanol and acetonitrile seem to dissociate into monomers as ascertained by the solution magnetic moment and mass spectrometry. Low intensity peaks in the ESI–MS show a small amount of dimer present, as well as monomer with solvent coordinated. Additionally, CV and EPR data indicate that there may be small amounts of dimer in solution (see Section 3.3). Unfortunately, due to solubility constraints in

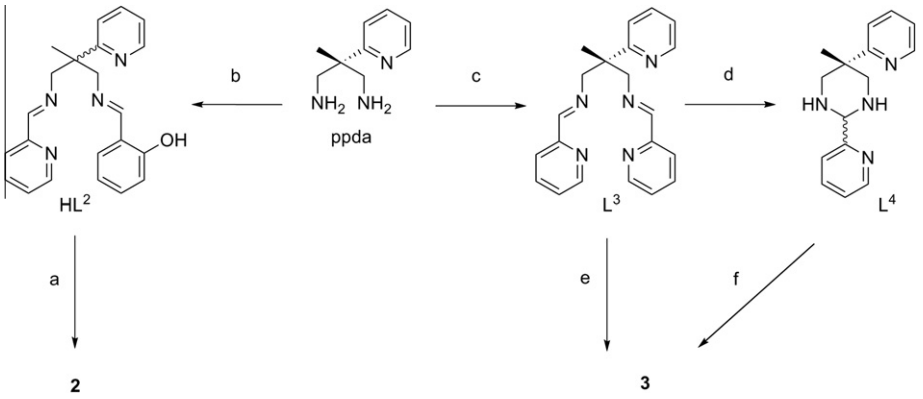

Scheme 1. Synthesis of HL^2, L^3, **2** and **3**. (a) $Cu(ClO_4)_2·6H_2O$; (b) 1 eq 2-pyridinecarboxladehyde, 1 eq 2-hydroxybenzaldehyde; (c) 2 eq 2-pyridinecarboxladehyde; (d) column chromatography on silica, or decomposition in solution; (e) $Cu(ClO_4)_2·6H_2O$ and (f) 1 eq 2-pyridinecarboxladehyde, $Cu(ClO_4)_2·6H_2O$.

non-coordinating solvent we were not able to study the nature of the dimer in solution.

Attempts to synthesize $[CuL^2]^+$ by the deprotonation of HL^2 were unsuccessful. The potentially monoanionic ligand HL^2 was treated with base either before or after the addition of copper(II) ions in order to investigate the formation of complexes with $(L^2)^-$. Addition of base to the ligand in methanol with subsequent complexation of copper(II) ions resulted in an accumulation of a mixture of a green and blue precipitate. According to mass spectrometry, complexes **2** and **3** were present in this mixture. Upon recrystallization of the crude powder, crystals of **3** were obtained. When complex **2** was treated with two equivalents of base (or water) in acetonitrile, no ligand rearrangement was observed according to mass spectrometry. Diffusion of diethyl ether into a solution of **2** in CH_3CN and NEt_3 did not form any crystalline material. The use of base before complex formation prohibits isolation of pure complex and leads to ligand rearrangement. Treatment of **2** with base to generate a copper(II) complex with $(L^2)^-$ were unsuccessful, despite HL^2 being stable towards decomposition and/or rearrangement of the arms when coordinated to the metal ion.

3.2. X-ray crystal structures

The previously published structure of **1** (Fig. 4) revealed that the copper ion was in a square pyramidal geometry with an N_2O_2 donor atom set from the $(L^1)^{2-}$ ligand in the equatorial plane and an axial O atom from a coordinated water molecule [22]. The pyridyl group does not coordinate in **1**, most likely due to geometric constraints that the bis(imine) ligand imposes on the complex. Compared to similar ligands with amine functional groups [36,37], the more planar geometry imposed to the ligand due to the imine C–N double bonds in **1** prevent the pyridyl N atom from folding into position where it can coordinate to the copper. This same constraint is seen in complexes **2** and **3** (vide infra).

According to the X-ray crystal structure of **2** (Fig. 5), each copper(II) ion in dimeric **2** is coordinated in a square pyramidal geometry with a τ_5 parameter [38] of 0.024 (Fig. 5). The N_3O donor atom set from the ligand occupies the basal plane of the pyramid with the μ_2-phenolato O atom from another complex coordinating in the apical position. The resulting structure contains two copper ions with bis(μ_2–O) bridging phenolate groups in a diamond core fashion. The apical O atom bond donor distance to the copper ion (Cu–O1#1 = 2.487 Å) is longer than the basal donors (ranging from 1.922–2.020 Å) due to the Jahn–Teller effect. The pyridyl ring from the ligand backbone is non-coordinating and, surprisingly, protonated at the N atom position. The overall +4 charge is balanced by four perchlorate counterions (Figure S6), two of which are weakly interacting with the copper(II) in the apical position *trans* to the phenolate O atom of each monomeric unit (Cu···O = 2.763 Å),

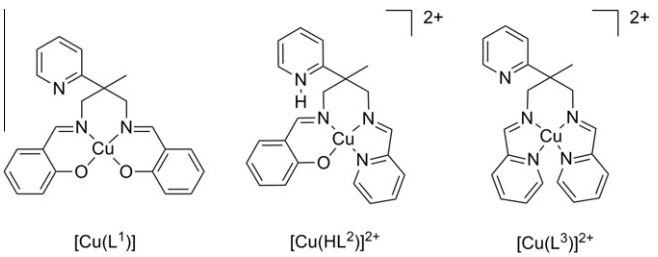

Fig. 3. Structures of the copper imine complexes discussed in this paper. The synthesis and structure of copper complex **1**, $[Cu(L^1)(CH_3OH)]$, was reported previously [22]. Complex **2**, $[Cu(HL^2)]_2(ClO_4)_4$, is a dimer in the solid state but is monomeric, e.g. $[Cu(HL^2)]^{2+}$, in solution. Complex **3**, $[Cu(L^3)](ClO_4)_2$, is a monomer in solution.

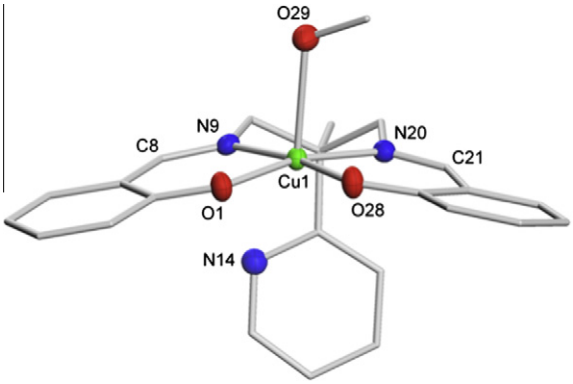

Fig. 4. Representation of the X-ray structure of **1** with H atoms removed for clarity. Reprinted with permission from Ref. [22].

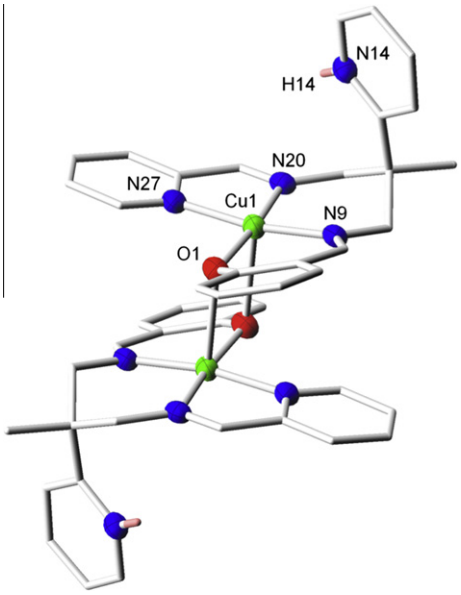

Fig. 5. Representation of the X-ray structure of the cationic portion of **2** with all H atoms except for the protonated pyridyl NH protons removed for clarity. Perchlorate anions and methanol solvent of crystallization molecules are also removed for clarity. Symmetry information used to generate equivalent positions: $(-x+½, -y+½, -z)$.

while the other two are non-coordinating. Hydrogen bonding between the pyridinium hydrogen and the non-coordinating methanol oxygen atom (N14–H14···O1S), as well as between the perchlorate ion oxygen and the methanol hydrogen atom (O1S–H1S···O1A#2), stabilizes the structure in the solid state (Figure S6, Table 3).

A complex similar to **2** was reported by Lee and coworkers with the ligand *N*-(salicylidene)-*N*′-(2-pyridylaldene)propanediamine [17]. This ligand differs from HL^2 only in the absence of the methyl and pyridyl groups on the propylene backbone. Complex **2** adopts the same $Cu_2(\mu$-phenolato$)_2$ diamond core, and has the same N_2O donor atom set as the complex with *N*-(salicylidene)-*N*′-(2-pyridylaldene)propanediamine [17]. Since HL^2 and *N*-(salicylidene)-*N*′-(2-pyridylaldene)propanediamine are effectively the same except for the pyridine group, both ligands coordinate in the same fashion, and the ligand–copper bond lengths and angles are very similar [17].

The X-ray structure of **3** consists of a mononuclear copper(II) complex of L^3 and two perchlorate anions (Fig. 6). The coordination geometry in **3** is axially elongated six-coordinate tetragonal. The L^3

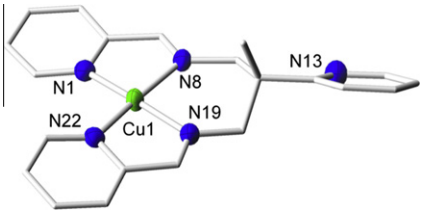

Fig. 6. Representation of the X-ray structure of the cationic portion of **3** with all H atoms removed for clarity. Perchlorate anions are also removed for clarity.

ligand coordinates in a slightly distorted square planar (τ_4 = 0.154) [39] manner while the perchlorate oxygens are weakly coordinating in the axial positions (Cu1–O1A = 2.660 Å and Cu1–O1B = 2.573 Å). As observed in other Cu(II) complexes with our bis(imine) family of ligands, here the ligand backbone pyridine nitrogen atom is non-coordinating. The geometrical constraints imposed by the ligand prevent the pyridyl ring from getting close enough to coordinate to the copper ion. As in **2**, there is significant bond elongation between the copper(II) ion and the axial donor atoms versus the donors in the basal plane.

A complex similar to **3** was reported by Ray and coworkers with the ligand *N*,*N*′-bis(2-pyridylaldene)propane-1,3-diamine [16]. Similar to HL^2 and its analog, L^3 and *N*,*N*′-bis(2-pyridylaldene)propane-1,3-diamine coordinate via the same N_4 donor atom set. Both complexes show the same N_4 coordination mode, with similar ligand–copper bond lengths and angles, due to the ligands sharing same ligand backbone and the fact that the pyridyl group of L^3 does not coordinate the the copper atom.

H_2L^1, HL^2 and L^3 have a common coordination mode to copper(II) ions. While the pyridine nitrogen atom of each ligand backbone is non-coordinating, the remaining N and O donors chelate in the basal plane around the metal ion (see Fig. 3). The pyridyl ring does not coordinate in **1**–**3** because of geometric constraints imposed by the rigid imine groups in H_2L^1, HL^2 and L^3. This stands in contrast to copper complexes of the more flexible series of bis(amine) ligands synthesized in our laboratory [36]. The geometry of **1** is similar to **2** but features a CH_3OH oxygen donor atom (not shown in Fig. 3) in the axial position rather than a bridging phenolate. Therefore, **1** is found as a monomeric species. Complex **2** and **1** show bond elongation in the axial positions (2.34 Å for $[Cu(L^1)(CH_3OH)]$ and 2.49 Å for **2**) compared to the basal donors, averaging in metal–ligand atom bond distances from 1.92 to 2.02 Å. Although **3** was synthesized in CH_3OH and crystallized from CH_3CN, no solvent molecule occupies the axial position. Instead, perchlorate anions are found in weak association to the metal ion in the axial positions (2.57 and 2.66 Å).

3.3. Spectroscopic and electrochemical characterization

Electrospray mass spectrometry suggests that CH_3OH and CH_3CN solutions of **2** dissociate mostly into monomeric species. A peak at m/z = 420.1 corresponding to $[Cu(L^2)]^+$, and a peak at m/z = 452.1 corresponding to $[Cu(L^2)(CH_3OH)]^+$ are indicative of monomeric species. A peak with very low intensity at m/z = 941.1 corresponding to $[(Cu(L^2))_2ClO_4]^+$ dimeric was also detected. This dissociative behavior in solution is further supported by a solution magnetic moment of 1.76 μB/Cu. This magnetic moment, which is close to the spin-only value of 1.73 μB/Cu, suggests the absence of any magnetic coupling and therefore supports the existence of a monomeric species in solution.

Frozen solutions of compound **2** in methanol show EPR spectra with two sets of peaks, which originate from two typical axial EPR signals (Figure S7, blue). Those two sets of signals most likely correspond to monomeric and dimeric forms of **2**. Due to differences in the coordination environment around the copper ions between the monomer and the dimer, we expect to see differences in *g* values and therefore two sets of axial EPR signals. To further support our hypothesis we allowed solutions of **2** to equilibrate in a dry ice/acetone bath for 2 h before freezing the sample in liquid nitrogen. The corresponding EPR spectrum (Figure S7, red) only shows one set of signals which would be expected to see for only one species, which we believe is dimeric **2**.

Frozen solutions of **2** in CH_3CN only show one axial EPR signal. Complex **2** has a much greater solubility in CH_3CN than in CH_3OH and due to the solubilty difference it is reasonable to assume that **2** dissociates immediately in CH_3CN. The slight shift in g for the monomers is likely due to solvent coordination (CH_3OH versus CH_3CN).

CH_3CN solutions of **3** were found to contain monomeric species, as ascertained by electrospray mass spectrometry (m/z = 505, corresponding to $[Cu(L^3)ClO_4]^+$) and solution magnetic moment measurements (1.75 μB/Cu). Complex **3** likewise possesses an axial EPR spectrum.

The redox behavior of **2** and **3** were studied by cyclic voltammetry and compared to the previously reported electrochemical parameters for **1** [22] (Fig. 7). The cyclic voltammograms (CVs) show reversible one-electron redox couples with $E_{1/2}$ = –1099 mV versus Fc/Fc^+ and ΔE = 77 mV for **2**, and $E_{1/2}$ = –438 mV versus Fc/Fc^+ and ΔE = 64 mV for **3**. The CV of **2** is complicated by a small reduction feature immediately before the E_{pc} peak that disappears on successive scans (this unusual redox behavior is undergoing further study). The CV in Fig. 7 is therefore the second scan, and the full first-scan CV of **2** is shown in Figure S8. Additional redox features in the CV are most likely due to some dimeric species. The redox couples, which were measured in CH_3CN, were assigned to the Cu(II)/Cu(I) pair. In contrast, the previously synthesized complex **1** exhibits its redox couple, which was measured in CH_2Cl_2, at $E_{1/2}$ = –1585 mV and ΔE = 136 mV. The CV for **1** in CH_3CN was measured and the $E_{1/2}$ was slightly lower than it was in CH_2Cl_2, with $E_{1/2}$ = –1489 mV and ΔE = 93 mV. The potential needed to reduce the copper(II) ion is most negative for the bis(phenol)bis(imine), **1**, followed by the hybrid bis(imine) **2**, and finally the most positive for the bis(pyridyl)bis(imine) **3**, all differing by about half of a volt. This trend can be explained by the electronic nature of the ligands. H_2L^1, being the most electron donating as the dianionic $(L^1)^{2-}$, stabilizes the copper ion in the higher oxida-

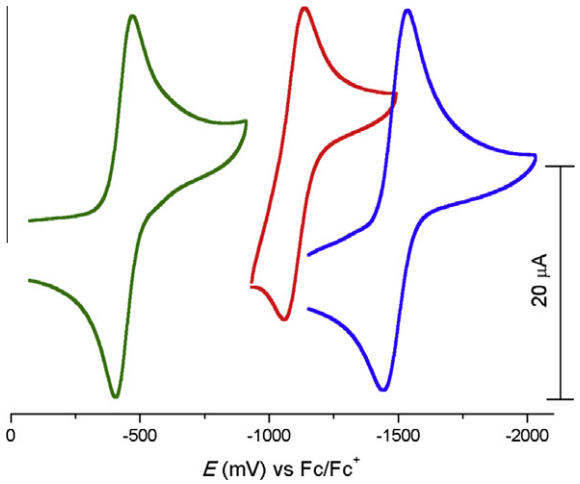

Fig. 7. Cyclic voltammograms (scan rate = 100 mV s^{-1}; 0.1 M $TBAPF_6$ supporting electrolyte) of 1.0 mM CH_3CN solutions of **1** (blue), **2** (red) and **3** (green). (For interpretation of the references to colour in this figure legend, the reader is referred to the web version of this article.)

Table 4
Electrochemical data for complexes **1**–**3** and literature complexes containing similar ligand sets.[a]

Complex	$E_{1/2}$ (V)	ΔE (mV)	i_{pc}/i_{pa}	Solvent	References
1	−1.585	136	0.99	CH_2Cl_2	[22]
1	−1.489	93	1.19	CH_3CN	This work
McMillin [$Cu(N_2O_2)$] complex	−1.300	325		DMF	[40]
2	−1.099	77		CH_3CN	This work
McMillin [$Cu(N_3O)$] complex	−0.932	280		DMF	[40]
3	−0.438	64	1.06	CH_3CN	This work
Nakahara [$Cu(N_4)$] complex	−0.550			DMF	[18]
McMillin [$Cu(N_4)$] complex	−0.526	150		CH_3CN	[40]

[a] All potentials referenced to the *Fc*/*Fc*$^+$ redox couple. CVs for solutions of **1**–**3** (1.0 mM) were recorded using a glassy carbon electrode with scan rates of 100 mV s^{-1}, and with 0.1 M $TBAPF_6$ supporting electrolyte.

tion state and disfavors reduction of the copper(II) ion. On the other extreme, the neutral L^3 ligand is the least electron donating ligand, which results in favorable acceptance of an electron by the metal ion to form a cuprous species and a less negative $E_{1/2}$.

The same trend with similar absolute redox potentials for the $Cu^{II/I}$ couple was observed on related Cu(II) complexes by McMillin and coworkers [40]. In their study, copper(II) complexes of the Schiff bases *N*,*N*′-bis(salicylidene)propane-1,3-propanediamine (N_2O_2 donor), *N*-(salicylidene)-*N*′-(2-pyridylaldene)-1,3-propanediamine (N_3O donor) and *N*,*N*′-bis(2-pyridylaldene)-1,3-propanediamine (N_4 donor) were prepared and the copper-centered redox couple determined through cyclic voltammetry. For comparison with our data (see Table 4) these potentials were corrected to the ferrocene/ferrocenium reference (*Fc* = 0.312 V versus SSCE) [41].

The difference in potential between our N_2O_2-donor complex, **1**, and the copper(II) complex with McMillin's ligand [40] is 285 mV. For the N_3O set, despite the fact that our complex has a ClO_4^- as the counterion while McMillin's complex has a NO_3^- counterion, the potentials are less than 100 mV different. Similarly, the redox potentials for the N_4 complexes are very similar. The N_4 copper(II) complex of *N*,*N*′-bis(2-pyridylaldene)-1,3-propanediamine was synthesized and characterized by Nakahara as well [18]. The redox potential for their complex was measured against SCE, and in order to compare to our complex it was corrected to be versus ferrocene/ferrocenium (*Fc* = 0.470 V versus SCE in DMF, [NBu_4][ClO_4]) [42]. Nakahara and coworker's reported electrochemistry matches nicely with McMillin's, even though it was measured in a different solvent. The relatively minor differences ranging from 100 to 285 mV between our complexes and ones in the literature may be due to the differences in substitution of the propanediamine backbone. In general, it is difficult to compare redox potentials directly due to errors in conversion to different references/electrodes and systems, but the overall trends are in good agreement.

4. Conclusions

In summary, two new copper(II) complexes, **2** and **3**, were synthesized using tetradentate Schiff base ligands HL^2 and L^3, respectively. Complexes **2** and **3** were compared with our previously synthesized copper(II) complex, **1**, which contains related tetradentate Schiff base ligand H_2L^1. Structurally, **1**–**3** are very similar, with the ligand coordinating to the square pyramidal copper center in the equatorial square plane. The ligand in complex **1** (H_2L^1), which is deprotonated at the phenol group, coordinates through the two imine N atoms and two phenolate O atoms. Complex **2** is coordinated by one pyridyl and two imine N atoms, and one phenolate O atom, also in the equatorial plane of the square pyramid. While the axial ligand in **1** is a coordinated methanol molecule, a bridging phenolate O atom sits in the axial position of **2**, forming a dimer. Complex **3** is coordinated by two pyridyl and two imine N atoms in the equatorial plane, having weakly coordinated perchlorate anions in the axial positions. The ligands in all three complexes do not coordinate through the pyridine nitrogen of the ligand backbone. The inability of the pyridyl group from the ligand backbone to coordinate is likely due to steric and geometric constraints of the rigid imine skeletons of the ligands. The electrochemical properties of **1**–**3** were probed by cyclic voltammetry, showing a correlation of the electronic properties of the ligands to the redox potentials of the cupric/cuprous ion couple. The more electron rich, dianionic $(L^1)^{2-}$ ligand in **1** with its N_2O_2 donor atom set highly favors the +2 oxidation state and has the most negative redox potential. The neutral L^3 ligand with its N_4 donor atom set has a redox potential that is more than a volt more positive, while the mixed ligand HL^2 with its N_3O donor atom set is midway between the other two. The electrochemical trends observed for **1**–**3** conform with the electrochemical properties of copper(II) complexes with similar ligands [18,40].

Acknowledgements

This work was supported by the National Science Foundation (NSF CHE-0616941) and the University of Oklahoma. Additionally, we thank the NSF for the purchase of a CCD-equipped X-ray diffractometer (CHE-0130835).

Appendix A. Supplementary material

^{1}H NMR spectra of ligands H_2L^1, HL^2, L^3 and L^4 (Figs. S1–S5), X-ray structure highlighting H-bonding and intermolecular interactions in 2 (Fig. S6), EPR spectra of **2** in CH_3CN and CH_3OH (Fig. S7), and cyclic voltammogram of **2** (Fig. S8). CCDC 864524 and 864525 contain the supplementary crystallographic data for complexes **2** and **3**, respectively. These data can be obtained free of charge from The Cambridge Crystallographic Data Centre via http://www.ccdc.cam.ac.uk/data_request/cif. Supplementary data associated with this article can be found, in the online version, at http://dx.doi.org/10.1016/j.ica.2012.08.026.

References

[1] E.I. Solomon, R.G. Hadt, Coord. Chem. Rev. 255 (2011) 774.
[2] N. Roy, S. Sproules, E. Bothe, T. Weyhermuller, K. Wieghardt, Eur. J. Inorg. Chem. (2009) 2655.
[3] W. Yang, D.M. Du, Eur. J. Org. Chem. (2011) 1552.
[4] D.B. Rorabacher, Chem. Rev. 104 (2004) 651.
[5] M. Hirotsu, N. Kuwamura, I. Kinoshita, M. Kojima, Y. Yoshikawa, K. Ueno, Dalton Trans. (2009) 7678.
[6] A. Domenech, E. Garcia-Espana, S.V. Luis, V. Marcelino, J.F. Miravet, Inorg. Chim. Acta 299 (2000) 238.
[7] M. Nishikawa, K. Nomoto, S. Kume, H. Nishihara, J. Am. Chem. Soc. 134 (2012) 10543.
[8] P. Comba, M. Kerscher, Coord. Chem. Rev. 253 (2009) 564.
[9] B.E. Bursten, J. Am. Chem. Soc. 104 (1982) 1299.
[10] D.M. Murphy, I. Caretti, E. Carter, I.A. Fallis, M.C. Gobel, J. Landon, S. Van Doorslaer, D.J. Willock, Inorg. Chem. 50 (2011) 6944.

[11] M. Orio, O. Jarjayes, H. Kanso, C. Philouze, F. Neese, F. Thomas, Angew. Chem., Int. Ed. 49 (2010) 4989.
[12] G.H. Clever, S.J. Reitmeier, T. Carell, O. Schiemann, Angew. Chem., Int. Ed. 49 (2010) 4927.
[13] T. Storr, P. Verma, R.C. Pratt, E.C. Wasinger, Y. Shimazaki, T.D.P. Stack, J. Am. Chem. Soc. 130 (2008) 15448.
[14] T. Glaser, M. Heidemeier, J.B.H. Strautmann, H. Bogge, A. Stammler, E. Krickemeyer, R. Huenerbein, S. Grimme, E. Bothe, E. Bill, Chem. Eur. J. 13 (2007) 9191.
[15] M.K. Taylor, J. Reglinski, L.E.A. Berlouis, A.R. Kennedy, Inorg. Chim. Acta 359 (2006) 2455.
[16] M.S. Ray, R. Bhattacharya, S. Chaudhuri, L. Righi, G. Bocelli, G. Mukhopadhyay, A. Ghosh, Polyhedron 22 (2003) 617.
[17] C.-H. Kao, H.-H. Wei, Y.-H. Liu, G.-H. Lee, Y. Wang, C.-J. Lee, J. Inorg. Biochem. 84 (2001) 171.
[18] T. Sakurai, M. Kimura, A. Nakahara, Bull. Chem. Soc. Jpn. 54 (1981) 2976.
[19] L.C. Nathan, J.E. Koehne, J.M. Gilmore, K.A. Hannibal, W.E. Dewhirst, T.D. Mai, Polyhedron 22 (2003) 887.
[20] S. Chattopadhyay, M.G.B. Drew, A. Ghosh, Inorg. Chim. Acta 359 (2006) 4519.
[21] B. Sarkar, G. Bocelli, A. Cantoni, A. Ghosh, Polyhedron 27 (2008) 693.
[22] R. Shakya, A. Jozwiuk, D.R. Powell, R.P. Houser, Inorg. Chem. 48 (2009) 4083.
[23] S. Friedrich, M. Schubart, L.H. Gade, I.J. Scowen, A.J. Edwards, M. McPartlin, Chem. Ber./Recl. 130 (1997) 1751–1759.
[24] D.F. Evans, J. Chem. Soc. (1959) 2003.
[25] SMART Software Reference Manual, Bruker-AXS, Madison, WI, USA, 1998.
[26] SAINT Software Reference Manual, Bruker-AXS, Madison, WI, USA, 1998.
[27] G.M. Sheldrick, SADABS Program for Empirical Absorption Correction of Area Detector Data, University of Gottingen, Germany, 2002.
[28] G.M. Sheldrick, SHELXTL Version 6.10 Reference Manual, Bruker AXS Inc., Madison, Wisconsin, USA, 2000.
[29] International Tables for Crystallography, vol. C, Kluwer, Boston, 1995.
[30] R. Atkins, G. Brewer, E. Kokot, G.M. Mockler, E. Sinn, Inorg. Chem. 24 (1985) 127.
[31] E. Kwiatkowski, M. Kwiatkowski, Inorg. Chim. Acta 117 (1986) 145.
[32] H.Y. Luo, P.E. Fanwick, M.A. Green, Inorg. Chem. 37 (1998) 1127.
[33] H.Y. Luo, J.M. Lo, P.E. Fanwick, J.G. Stowell, M.A. Green, Inorg. Chem. 38 (1999) 2071.
[34] A. Biswas, M.G.B. Drew, A. Ghosh, Polyhedron 29 (2010) 1029.
[35] J.M. Locke, R. Griffith, T.D. Bailey, R.L. Crumbie, Tetrahedron 65 (2009) 10685.
[36] R. Shakya, Z.D. Wang, D.R. Powell, R.P. Houser, Inorg. Chem. 50 (2011) 11581.
[37] M. Schmidt, D. Wiedemann, A. Grohmann, Inorg. Chim. Acta 374 (2011) 514.
[38] A.W. Addison, T.N. Rao, J. Reedijk, J. van Rijn, G.C. Verschoor, J. Chem. Soc., Dalton Trans. (1984) 1349–1356, http://dx.doi.org/10.1039/DT9840001349.
[39] L. Yang, D.R. Powell, R.P. Houser, Dalton Trans. (2007) 955.
[40] R.C. Elder, E.A. Blubaugh, W.R. Heineman, P.J. Burke, D.R. McMillin, Inorg. Chem. 22 (1983) 2777.
[41] H. Nishihara, Advances in Inorganic Chemistry 53 (53) (2002) 41.
[42] D. Chang, T. Malinski, A. Ulman, K.M. Kadish, Inorg. Chem. 23 (1984) 817.